No	Materials	Wavelength of excitation	Produce $O_2^{\cdot-}$	Produce •OH	Produce $^1O_2$	Ref
1	TiO_2-ruthenium complex (N3)	UV and visible light	✓	✓	✓	Angew. Chem. Int. Ed. 2017, 56, 10717
2	π-conjugated small molecule (COi6-4Cl)	880 nm	✓	×	✓	Adv. Mater. 2020, 32, 2003471
3	Nile blue derivative (ENBO)	660 nm	✓	×	×	J. Am. Chem. Soc. 2019, 141, 2695
4	π-conjugated small molecule (BthB)	808 nm	✓	×	✓	Nanoscale, 2021, 13, 8012
5	Aggregation-induced emission (AIE) molecule	Visible light	✓	✓	✓	ACS Appl. Mater. Interfaces 2022, 14, 5112
6	π-radical molecule (PTM-TPA)	635 nm	✓	×	✓	Mater. Horiz. 2021, 8, 571
7	Carbon dots	405 nm	✓	×	NA	Matter 2020, 2, 495.
8	AIE molecule	Visible light	✓	NA	✓	Adv. Funct. Mater. 2020, 30, 2002057
9	Supramolecule (HG)	580 nm	✓	NA	✓	Chem. Sci. 2022, 13, 5951
10	Nitroxide radical (NDIT)	635 nm	✓	✓	✓	This work

Table 1. Comparison of NDIT with other reported type-I agents.

Synthesis and Molecular Structure Characterization Data

Compound NDI-Br. ^{1}H NMR (400 MHz, $CDCl_3$) δ 10.41 (t, J = 5.3 Hz, 1H), 8.88 (s, 1H), 8.44 (s, 1H), 4.12 (dd, J = 7.1, 5.0 Hz, 4H), 3.88 (t, J = 4.9 Hz, 2H), 3.84-3.76 (m, 4H), 3.73-3.61 (m, 2H), 1.96 (s, 2H), 1.23 (s, 50H), 0.85 (t, J = 6.4 Hz, 12H).

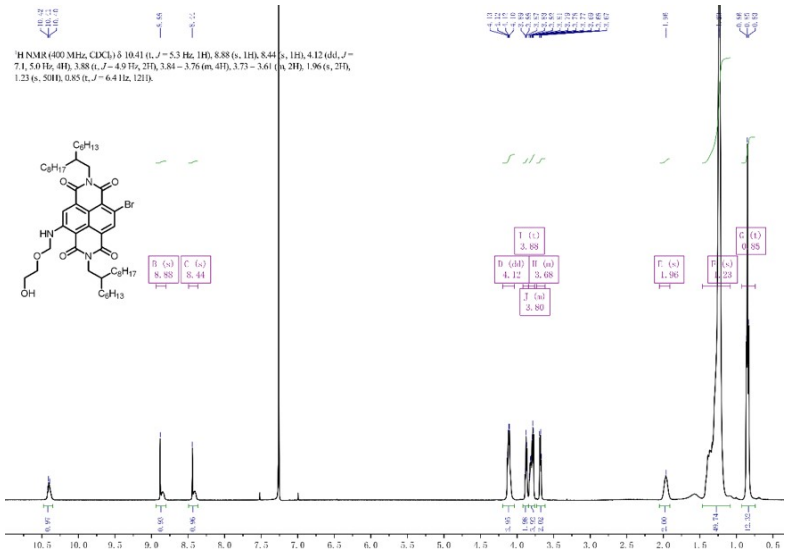

Figure S1. NMR spectrum of compound NDI-Br.

Compound NDI-TEMPO. ^{1}H NMR (400 MHz, $CDCl_3$) δ 9.76 (s, 1H), 8.33 (s, 1H), 4.14 (s, 5H), 4.03 – 3.62 (m, 10H), 2.80 (s, 1H), 2.02 (s, 2H), 1.28 (s, 62H), 0.89 (s, 15H).

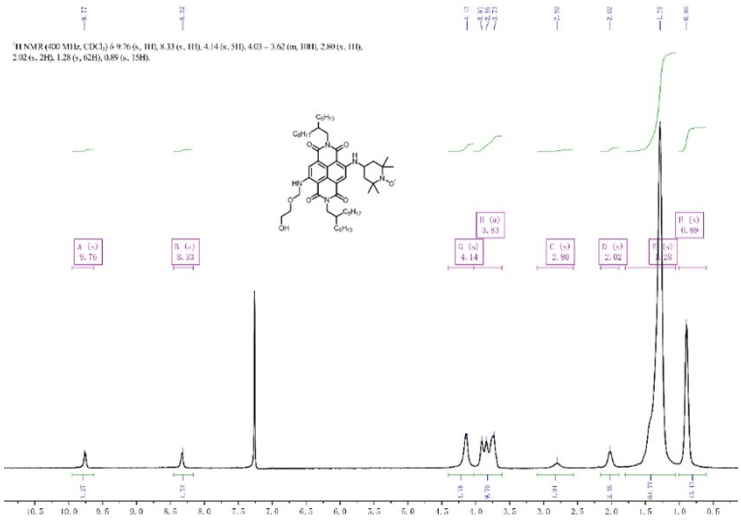

Figure S2. NMR spectrum of compound NDI-TEMPO.

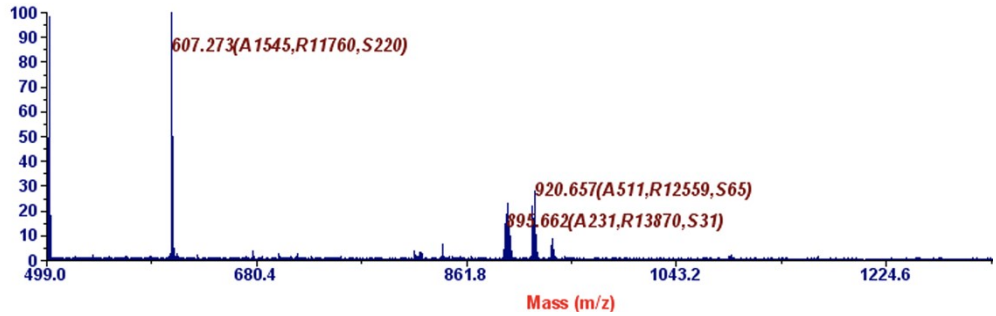

Figure S3. Mass spectrometry of compound NDI-Br.

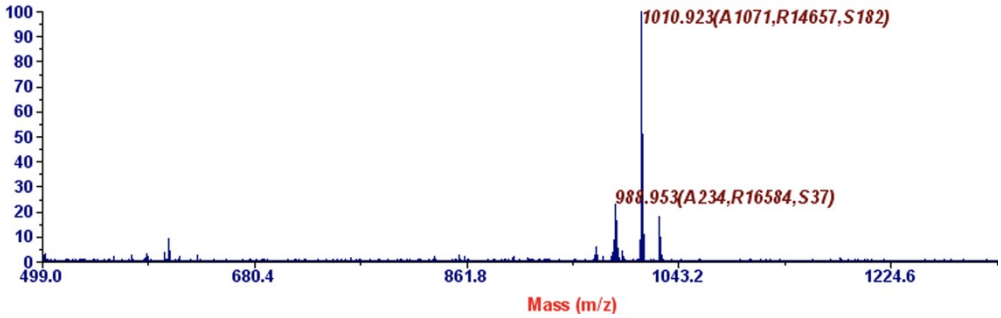

Figure S4. Mass spectrometry of compound NDI-TEMPO.

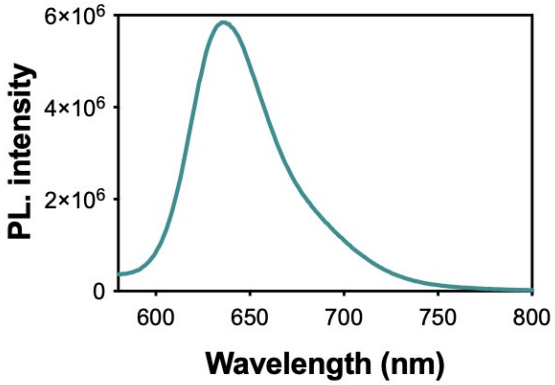

Figure S5. Fluorescence spectrum of aqueous NDIT molecule in tetrahydrofuran (THF).

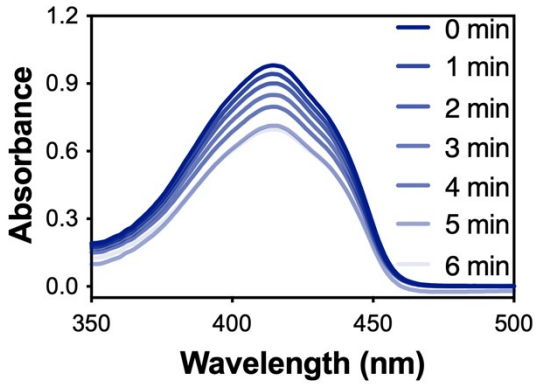

Figure S6. Time-dependent absorption spectra of DPBF in the presence of MB molecule under 635 nm irradiation.

Figure S7. Image of NDIT NPs dispersed in different media.

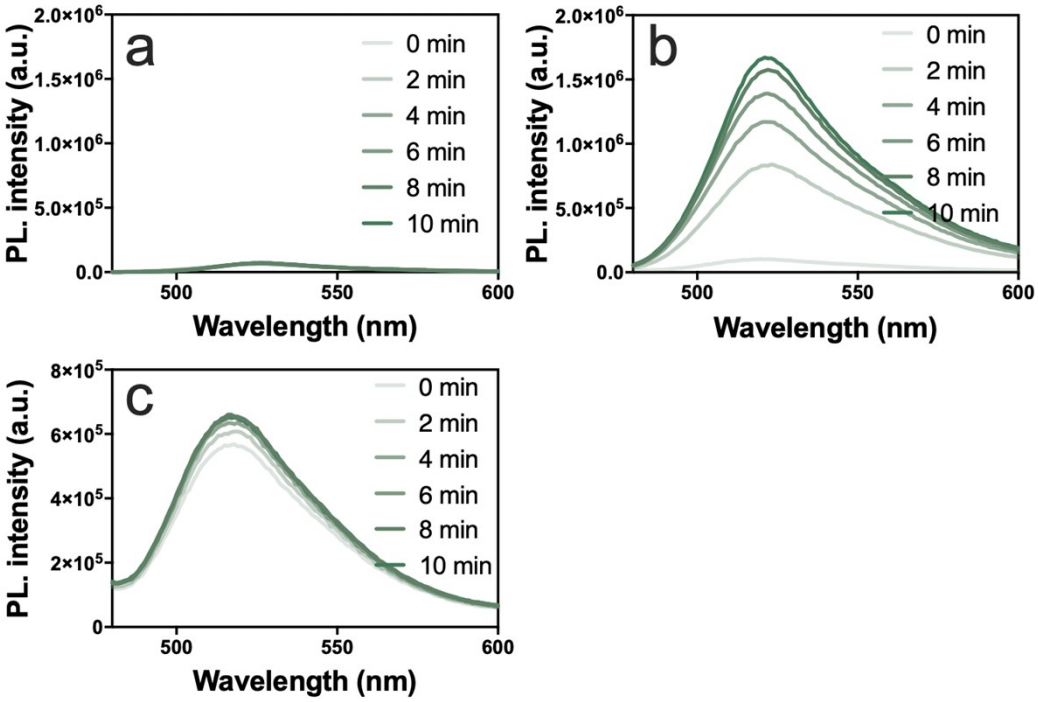

Figure S8. SOSG spectra after addition of (a) only water, (b) NDIT NPs (50 μg/mL) without removing oxygen and (c) NDIT NPs (50 μg/mL) after removing oxygen.

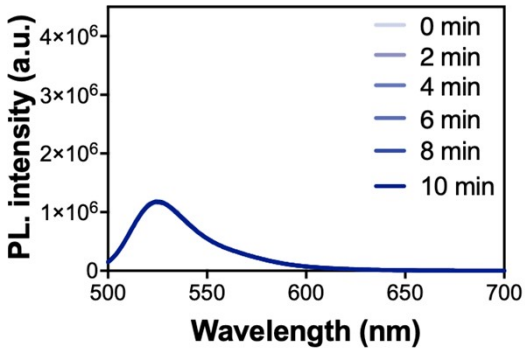

Figure S9. DHR123 spectra of control group (only water) after removing oxygen.

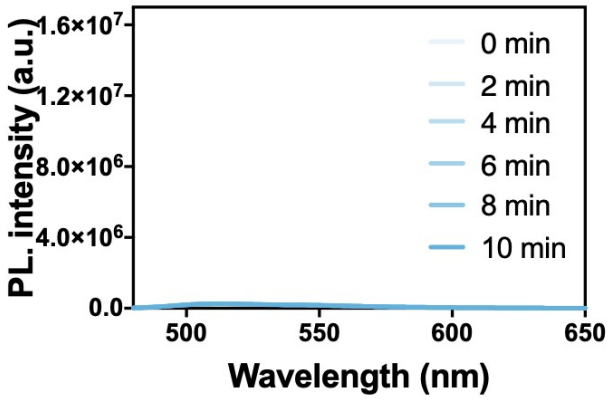

Figure S10. HPF spectra of control group (only water) after removing oxygen.

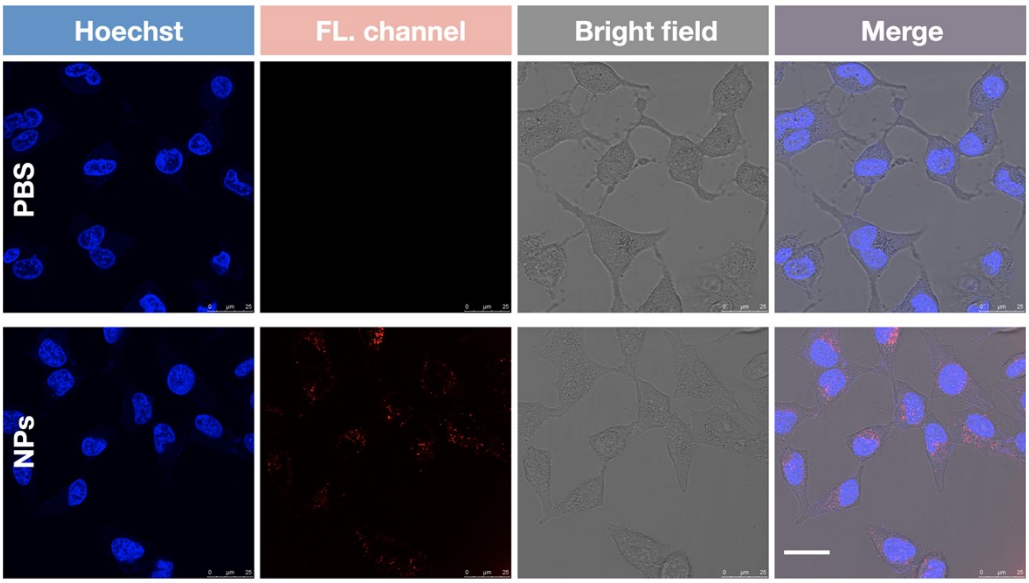

Figure S11. HeLa cell imaging of NPs, scale bar is 25μm.

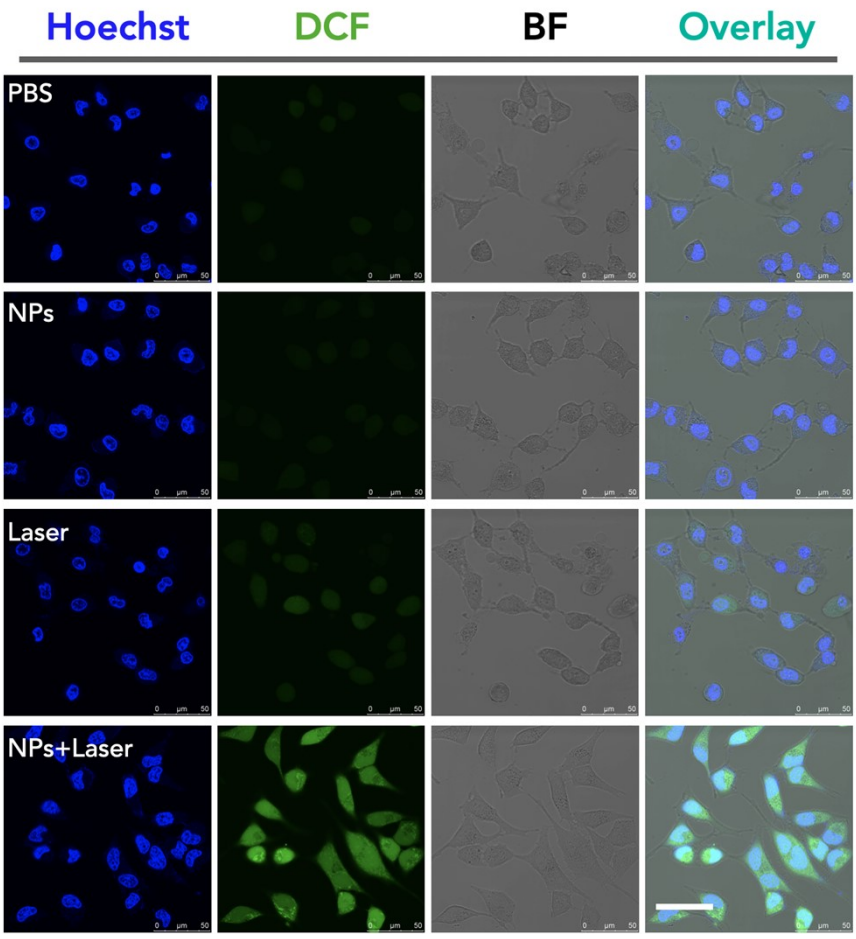

Figure S12. Fluorescence images of DCF in HeLa cells after different treatments, Hoechest 33342 is for nuclei staining. Scale bar is 50 μm.

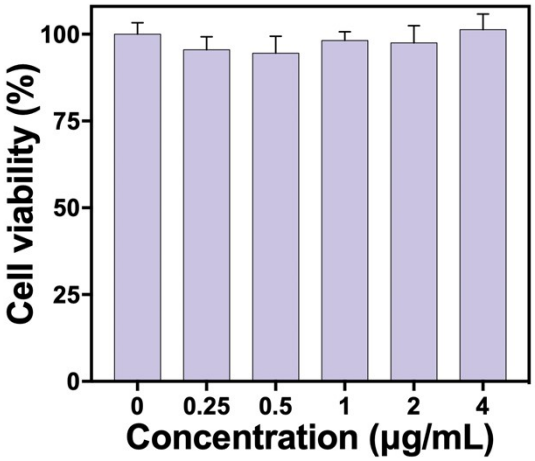

Figure S13. Healthy cell viability (3T3) of NPs in dark after 24 h's incubation.

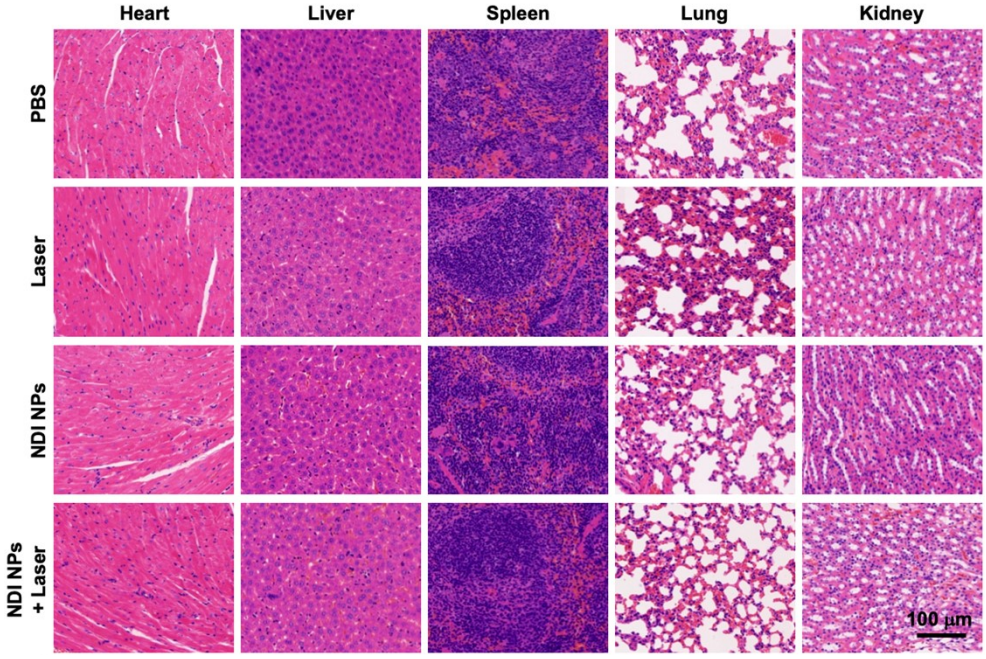

Figure S14. H&E staining of major organs from mice in different groups. Scale bar =100 μm.

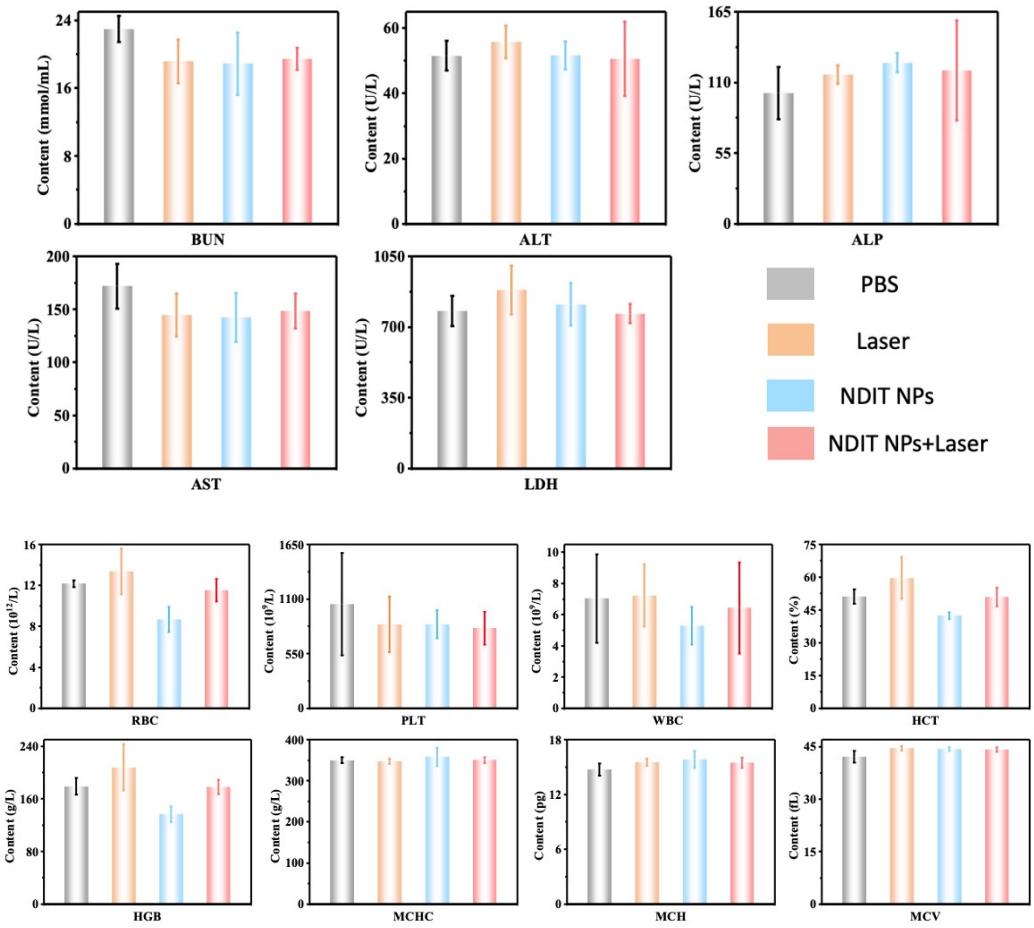

Figure S15. Blood routine test and biochemistry analysis of mice after various treatments.

Materials: Amphiphilic polymer DSPE-PEG 2000 was acquired from Avanti Polar Lipids. Cell Counting Kit-8 (CCK8) was bought from Beyotime. Tetrahydrofuran (THF), dichloromethane (DCM), 2',7'-Dichlorofluorescin diacetate (DCFH-DA), Calcein acetoxymethyl ester (Calcein-AM), Propidium Iodide (PI), Dihydrorhodamine 123 (DHR 123) and 1,3-Diphenyliso-benzofuran (DPBF) were bought from Sigma-Aldrich. Fetal bovine serum (FBS), antibiotic agent penicillin-streptomycin (10 000 U mL^{-1}), Dulbecco's modified Eagle's medium (DMEM), PBS (pH 7.4, 10×), and trypsin-EDTA (no phenol red) were obtained from Thermo Fisher Scientific. Hydroxyphenyl fluorescein (HPF) was purchased from ENZO Life Science. Singlet

oxygen sensor green (SOSG), and Image-iT™ Green Hypoxia Reagent were purchased from Invitrogen. All chemicals were used without further purification.

Synthesis of molecules: A mixture of 4-bromo -2,7-bis(2-hexyldecyl)-9-((2-(2-hydroxyethoxy)ethyl)amino)benzo[lmn][3,8]phenanthroline1,3,6,8(2H,7H)-tetraone (67 mg, 0.1 mmol) and 4-amino-TEMPO (171 mg, 1mmol) in 2-methoxye-thanol (10 mL) in 20 ml 2-methoxyethanol for 3 days under argon atmosphere in a 120 ^{o}C oil bath with thin layer chromatography (TLC) monitoring. After removal of 2-me-thoxyethanol under reduced pressure, the residue was purified by column chromatography (silica gel, DCM/methanol= 100:1, v/v) to give 30 mg of a blue solid. Yield: 40%.

Preparation of nanoparticles (NPs): 500 μL NDIT radical molecule (0.5 mg/mL in THF) and 500 μL DSPE-PEG2000 (5mg/mL in THF) were fully mixed using ultrasonication and then added dropwise into 9 mL of stirring DI water under vigorous stirring. After 48 h, the as-prepared nanoparticles were collected with a 100,000 KDa ultrafiltration tube. The as-prepared solution was filtered and stored at 4 °C before future use.

Characterizations: NMR spectra were recorded in $CDCl_3$ by a Bruker Advance-600 spectrometer, and mass spectra data were achieved *via* Bruker autoflex MALDI-TOF mass spectrometer. Size and morphology of NPs were studied on transmission electron microscope (TEM, Philips CM-200 FEG). Size of NPs were measured using a Malvern Zetasizer Nano ZS. Absorption properties was obtained using a Shimadzu-1700 spectrometer. Photoluminescence (PL) spectra of molecules/NPs and probes were

explored by Edinburgh FLS 980 and Horiba Fluoromax-4 Spectrofluorometer. The phosphorescence of singlet oxygen was measured by Edinburgh FLS 980. ESR signal of molecule in THF and NPs in PBS were detected using the ESR technique without addition of any trapping agents (E500, Bruker). Leica TCS SPE/SP5 laser confocal scanning microscope were used for confocal fluorescence imaging. Fluorescence imaging was recorded on the IVIS Spectrum *in vivo* imaging system (PerkinElmer, U.S.).

Singlet oxygen detection: Singlet oxygen generation of NDIT molecule was determined by using DPBF. Typically, 700 μL of NDIT molecule solution (DCM) containing DPBF was exposed to a 635 nm laser (0.3 mW/cm^2) for 0, 10, 20, 30, 40, 50, and 60 second. MB dissolved in DCM was chosen as the reference PS. The initial DPBF absorbance was set at around 1.0, and the OD value of the NDIT molecule and MB molecule at 635 nm were set at around 0.2 OD. All samples were carefully protected from light and the absorbance of DPBF were measured.

Singlet oxygen detection by SOSG: $^1O_2$ generation in solution were monitored with SOSG via its fluorescence intensity. Briefly, SOSG (final concentration: 5 μM) was mixed with nanoparticles (final concentration: 50 μg/mL) and irradiated by 635 nm laser (0.1 W/cm^2). Then the fluorescence intensities at 525 nm of different irradiation intervals (0, 2, 4, 6, 8 and 10 min) were recorded upon the excitation of 460 nm.

$O_2^{-\bullet}$ detection in stimulated hypoxia. DHR 123 probe was used to detect $O_2^{-\bullet}$ generation via its fluorescence intensity change. Typically, DHR 123 (final concentration: 10 μM) was mixed with nanoparticles (final concentration: 50 μg/mL).

Next, oxygen in prepared solution was removed by quick freezing-defrosting-refreezing using liquid nitrogen for 3 times. After that, the mixtures were exposed to irradiation from a 635 nm laser (0.1 W/cm^2). Upon 460 nm excitation, the PL intensity of DHR 123 at 525 nm were measured at different irradiation intervals (0, 2, 4, 6, 8 and 10 min).

•OH detection in stimulated hypoxia. HPF probe fluorescence intensity was applied to detect •OH generation. Typically, HPF (final concentration: 10 μM) in PBS (pH 7.4) was mixed with nanoparticles (final concentration: 50 μg/mL). After that, the mixtures were exposed to irradiation from a 635 nm laser (0.1 W/cm^2). The PL intensity of HPF at 525 nm were measured at different irradiation intervals (0, 2, 4, 6, 8 and 10 min) upon 460 nm excitation.

ROS Generation Mechanism: Upon irradiation of 635 nm laser, doublet ground state (D_0) of NDIT radical was excited to its doublet excited state (D_1). When there is enough oxygen in the surrounding, it follows the type II mechanism *via* energy transfer towards O_2 for singlet oxygen generation ($^1O_2$). While in hypoxia, type II PDT mechanism will be strongly inhibited due to the low oxygen concentration. On the other hand, , type I PDT mechanism is not sensitive to the oxygen concentration. In a type I PDT reaction, the excited photosensitizer can directly transfer electrons to ambient O_2 to form superoxide radicals ($O_2^{-\bullet}$). $O_2^{-\bullet}$ will then react with superoxide dismutase (SOD) inside cells to form H_2O_2 and O_2 (Proc. Natl. Acad. Sci. U. S. A. **2015**, 112, 2343-2348; J. Am. Chem. Soc. **2020**, 142, 5177-5183; J. Am. Chem. Soc. **2018**, 140, 14851-14859; J. Am. Chem. Soc. **2018**, 140, 14851-14859). In the presence Fe^{2+}, H_2O_2 will then form

hydroxyl radical (•OH) which can kill cancer cells. As O_2 molecules are recycled instead of consumed, type I PDT reaction can be continuous even through there is very little oxygen in the initial environment.

***In Vitro* Cell Imaging**: To monitor the uptake of nanoparticles, the cells were seeded in 27 mm nunc glass base dish. Then the cells were incubated with nanoparticles (final concentration: 50 μg/mL) for 6 h. Fluorescence cells images were recorded with a Leica TCS SPE Spectral Confocal Microscope with 405 nm excitation.

Intracellular Hypoxia Evaluation: To induce intracellular hypoxia, we used deferoxamine (DFO). DFO enables chelating iron for excretion and stabilizing HIF-1alpha from proteolysis by inhibiting the activity of iron-dependent prolyl hydroxylases subsequently reducing the potential for O_2 transport (Adv. Mater. 2016, 28, 3313-3320; Nature 1999, 399, 271-275). Then, the DFO-treated cells were returned a cell incubator with 20% O_2, 5% CO_2 and 37 ^oC. Intracellular hypoxia was confirmed with the fluorescence intensity of Image-iT™ Green Hypoxia Reagent. It is non-fluorescent when live cells are in an environment with normal oxygen concentrations and becomes fluorescent when oxygen level is low. Image-iT™ Green Hypoxia Reagent (final concentration: 10 μM) was added in DMEM. After staining A549 cell for 30 min, the original culture medium was replaced by fresh medium containing 200 μM DFO and incubated for another 4 h. At last, intensity of green fluorescence was recorded on a Leica TCS SPE Spectral Confocal Microscope under 488 nm excitation.

Intracellular ROS Detection: Generation of ROS was detected by the fluorescence

intensity of DCFH-DA. 6.7 μl of nanoparticles (final concentration: 10 μg/mL) were added to 2 mL of DMEM and incubated with A549 cells for 6 h. Next, DCFH-DA (working concentration: 50 μM) and Hoechst 33342 (working concentration: 10 μg/mL) was added for another 30 min staining. Then A549 cells were irradiated by 635 nm laser (0.1 W/cm^2, 5 min) and washed with PBS for three times. At last, green emission from DCF excited by 488 nm was recorded on a Leica TCS SPE Spectral Confocal Microscope.

Intracellular Superoxide Radical ($O_2^{-\bullet}$) Detection: $O_2^{-\bullet}$ generation was decided by the fluorescence intensity of DHE. 6.7 μl of NDIT NPs (final concentration: 10 μg/mL) were added to 2 mL of DMEM and incubated with A549 cells for 6 h. Next, DHE (working concentration: 5 μM) was added for 30 min staining. Then, A549 cells were washed three times by PBS and were irradiated by 635 nm laser (0.1 W/cm^2, 5 min). At last, red emission from DHE after interaction with $O_2^{-\bullet}$ was recorded on a Leica TCS SPE Spectral Confocal Microscope using 488 nm excitation.

A549 Cytotoxicity by Cell Counting Kit-8 (CCK-8) Assay: Cell viability of the nanoparticles was evaluated by CCK-8 assay. 4 μl of DFO (final concentration: 200 μM) was incubated with A549 cells for 4 h to induce hypoxic environment. Then we replaced original medium with 200 μL DMEM containing different concentrations of (0 to 4 μg/mL). After incubation with A549 cells for 4 h, for PDT evaluation, NDIT NPs were irradiated with a 635 nm laser (0.1 W/cm^2, 30 min). The plates were then returned back to incubator for another 12 h incubation. Then, 10 μL of CCK-8 was diluted ten times with DMEM and was added to each plate. After about 3 h, cell

cytotoxicity was measured by the absorbance value at 460 nm using a BioTek Powerwave XS microplate reader.

***In vivo* antitumor activity and biosafety:** For investigating the therapeutic efficacy of NDIT NPs *in vivo*, the antitumor activity was evaluated on A549 tumor-bearing nude mice. A549 cells were subcutaneously injected around three weeks before commencing PDT treatment. When the tumors grew to ~100 mm^3 in volume, these mice were divided into four groups randomly with six mice in each group. Different formulations were divided into four groups including only PBS, only NDIT NPs, PBS+Laser, NDIT NPs+Laser, respectively. NDIT NPs (200 μL, 1 mg/mL) or PBS (200 μL) were administrated *via* tail intravenous injection. The mice were kept from light. After injection for 12 h, the tumor was irradiated by 635 nm laser (300 mW cm^{-2}, 10 min). During the whole PDT treatments, both body weights and tumor volumes of mice were recorded every two days. To further estimate the therapeutic effect and biosafety *in vivo*, the tumor tissue and major organs (heart, liver, spleen, lung, kidney) were harvested for H&E staining after 2 and 14 day-therapy, respectively. To further evaluate the safety of different formulations *in vivo*, the serum levels of urea nitrogen (BUN), alanine aminotransferase (ALT), alkaline phosphatase (ALP), aspartate transaminase (AST), and lactate dehydrogenase (LDH) were analyzed using a Chemray 800 Automated Chemistry Analyzer (Shenzhen Rayto Life and Analytical Sciences).